Supporting Information

Attomolar label-free detection of DNA hybridization with electrolyte-gated graphene field-effect transistors

Rui Campos[†,ζ], Jérôme Borme[†], Joana Rafaela Guerreiro[†], George Machado Jr[†,#], Maria Fátima Cerqueira[†,#], Dmitri Y Petrovykh[‡], and Pedro Alpuim[†,#,*]

[†] Department of Quantum and Energy Materials, INL – International Iberian Nanotechnology Laboratory, 4715-330, Braga, Portugal

[‡] Department of Life Sciences, INL – International Iberian Nanotechnology Laboratory, 4715-330, Braga, Portugal

[#]CFUM – Center of Physics, University of Minho, 4710-057, Braga, Portugal

MATERIALS AND METHODS

Graphene transfer A layer of PMMA 950k (AR-P 679.04, Allresist, Germany) is spin-coated on top of the top side of the copper covered in graphene. The layer of graphene on the bottom side is removed by oxygen plasma. The copper is dissolved in iron chloride 0.5 M at 35 °C. The floating graphene and its temporary PMMA substrate are cleaned in a solution of hydrochloric acid 2 % for 30 min and rinsed into de-ionised water (resistivity ≥ 18 MΩ) for 5 minutes. The cleaning and rinsing procedures are repeated five times. Graphene is then transferred onto the pre-patterned substrate. In order to improve the removal of water between the wafer and graphene, the wafer is first submitted to a hydrophobic priming using vapor HDMS. The transferred graphene is dried in oven at 180 °C for 12 hours. After cooling down, the wafer is placed in an acetone bath for 2 hours to remove PMMA.

Electrochemical Measurements Capacitance measurements were performed using a Autolab 302N potentiostat running NOVA 2.1 software. The working electrode was a microelectrode array with 60 microelectrodes of 40 µm diameter and a distance between microelectrodes of 400 µm in a hexagonal arrangement. The reference and counter electrodes were, respectively, Ag/AgCl 3 M KCl from metrohm and a platinum flag of 1 cm^2. The electrochemical area determination was performed in a chip to which graphene had not been transferred, cyclic voltammetry was performed in 0.1 M H_2SO_4. The capacitance was determined from electrochemical impedance

spectroscopy measurements performed in PB 10 mM, in a range of potentials between -0.5 V and 0.5 V *vs.* Ag/AgCl with 50 mV intervals with each measurement being performed in a range of frequencies (100 kHz to 1Hz, amplitude 5 mV).

Raman Characterization. The EGFET channel has been characterized/monitored after each functionalization step by Confocal Raman spectroscopy measurements, performed at room temperature in a back scattering geometry, on a WITec Alpha300 R confocal Raman microscope using a 532 nm Nd:YAG laser for excitation, at an output power of 1.5 mW, and an objective ×50 lens (Zeiss, NA=0.7). The spectra were collected with a 600 groove/mm grating using 5 acquisitions with 2 s acquisition time. After stage 2 of the functionalization process (PBSE immobilization), a 633 nm excitation line from a He-Ne laser was also used. After each step multiple Raman measurements were performed in different points of the channel to confirm that the spectra acquired were representative.

Biosensor Development.

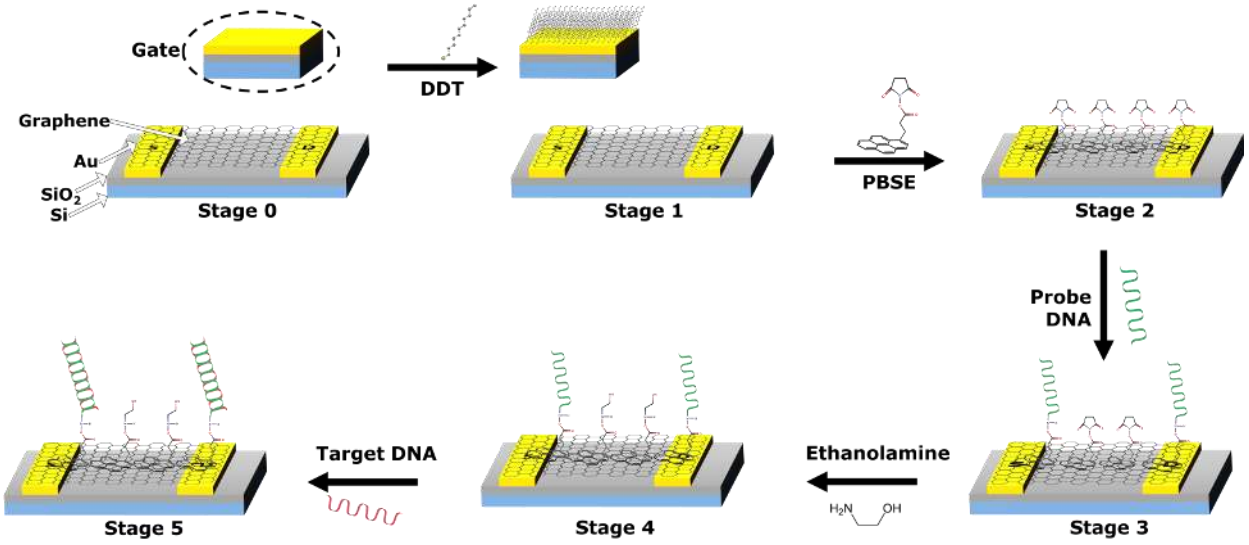

Figure S1. Schematic view of the stages of the biosensor development: Stage 0: as-fabricated graphene transistor; Stage 1: DDT gate passivation; Stage 2: immobilization of the linker (PBSE); Stage 3: functionalization with probe DNA; Stage 4: blocking with ethanolamine; Stage 5: biorecognition.

QCM-D experiments. Quartz crystal microbalance with dissipation (QCM-D) was used for *in situ* characterization of the immobilization of DNA probes and of the subsequent DNA hybridization on model graphene surfaces prepared following protocols similar to those used for the EGFET device.

The QCM measurements were performed in a QSense E1 system (Biolin Scientific). AT-cut quartz crystals having gold electrodes of the working surface coated with ca. 50 nm of silicon oxide (QSX 335, Biolin Scientific) were used as substrates for single-layer graphene transfer. QCM measurements for the fundamental (ca. 4.95 MHz) frequency and at its 6 odd overtones (n = 3, 5, 7, 9, 11, 13) were carried out under a flow rate of ca. 0.075 ml/min at a constant temperature of 20 °C (set within <1 °C from RT, at which the solutions have been stabilized prior to the measurements). The measurements produced consistent results in experiments on two different QCM crystals.

A QCM sensor with silicon oxide surface first was cleaned in a 1% Alconox solution at 60 ºC for 1 h followed by rinsing in deionized water and isopropanol. After cleaning the sensor in oxygen plasma, graphene was transferred onto the sensor surface following a procedure analogous to that used for EGFETs. Prior to QCM-D measurements, the graphene surface was modified with PBSE heterobifunctional linker (10 mM in DMF for 2 h) and then placed inside the QCM-D chamber.

After achieving a stable baseline with the running buffer 0.99 M $CaCl_2$-TE (1× TE buffer is 10 mM Tris·HCl and 1 mM EDTA) at a flow rate of 0.075 ml/min, 1 ml of the 25-nt DNA probe solution (1 μM in 0.99 M $CaCl_2$-TE) was recirculated through the chamber and allowed to react for ca. 30 min followed by a rinse in the blank running buffer to remove non-specifically bound DNA probes. Blocking the surface with ethanolamine (100 mM at pH 8 in water for 30 min) was performed outside the QCM chamber. After remounting the sensor in the chamber, a new baseline was collected and 1 mL of the DNA target (25-nt perfect match to the probe) solution (1 μM in 0.99 M $CaCl_2$-TE was recirculated through the chamber and allowed to react for ca. 30 min followed by a rinse in the blank running buffer to remove non-specifically bound DNA targets.

Specificity of the DNA probe immobilization and of the target recognition was evaluated in control experiments whereby: (1) the target (i.e., sequence of the same length and similar composition, but without the terminal amine modification) was used instead of the probe; (2) probe immobilization was attempted onto a surface after ethanolamine blocking; (3) the probe was used instead of the target, to simulate a non-complementary target sequence.

The surface density of DNA was estimated by using the Sauerbrey equation (Eq. 1):

$$\Delta m = -C \cdot \Delta f / n, \quad \text{(Eq. 1)}$$

where C is the mass sensitivity constant (C = 18.1 $ng \cdot cm^{-2} \cdot Hz^{-1}$ for the employed QCM sensors), n is the overtone number, Δm is the adsorbed mass per unit area ($ng \cdot cm^{-2}$), and Δf is the measured frequency shift (Hz).

XPS experiments. The chemical immobilization of the amine-modified simulated-probe DNA sequence (30-nt) was also investigated by x-ray photoelectron spectroscopy (XPS). Silicon surfaces with a thick silicon oxide layer were used as substrates, on which the graphene transfer and subsequent modification steps were carried out analogously to those on the QCM sensors described above. A simulated probe sequence, a 30-nt thymine homo-oligonucleotide (T_{30}), was used instead of the pDNA sequence to produce an XPS signature that is easier to interpret in terms of surface density and conformation of the surface-immobilized DNA strands.

Representative graphene surfaces before and after functionalization with PBSE and simulated-probe DNA were characterized in an ESCALAB 250 Xi system (Thermo Scientific) using a nonmonochromated Al Kα X-ray source, with an analyzer-defined analysis spot of <1 mm^2. Peak fitting was performed in Avantage instrument software (Thermo Scientific), choosing a minimal number of components that produced random residuals consistently for all the samples; a convolution of Gaussian and Lorentzian line shapes was used for all the spectral components. To avoid differential charging possible on the substrates with a thick layer of silicon oxide, uniform charge neutralization was provided by beams of low-energy (≤10 eV) Ar^+ ions and electrons guided by a magnetic lens; consistent charge neutralization was verified by observing the adventitious C 1s peak at 284.7±0.1 eV and the oxide substrate Si $2p_{3/2}$ peak at 103.7±0.1 eV for all samples. The position of the Si $2p_{3/2}$ component could be monitored because silicon oxide substrate in these measurements was of sufficient quality to exhibit the asymmetry due to the doublet structure, with FWHM of 1.5±0.1 eV for each of the spin-orbit components in the fits (Figure S5).

RESULTS

Transfer curve measurements

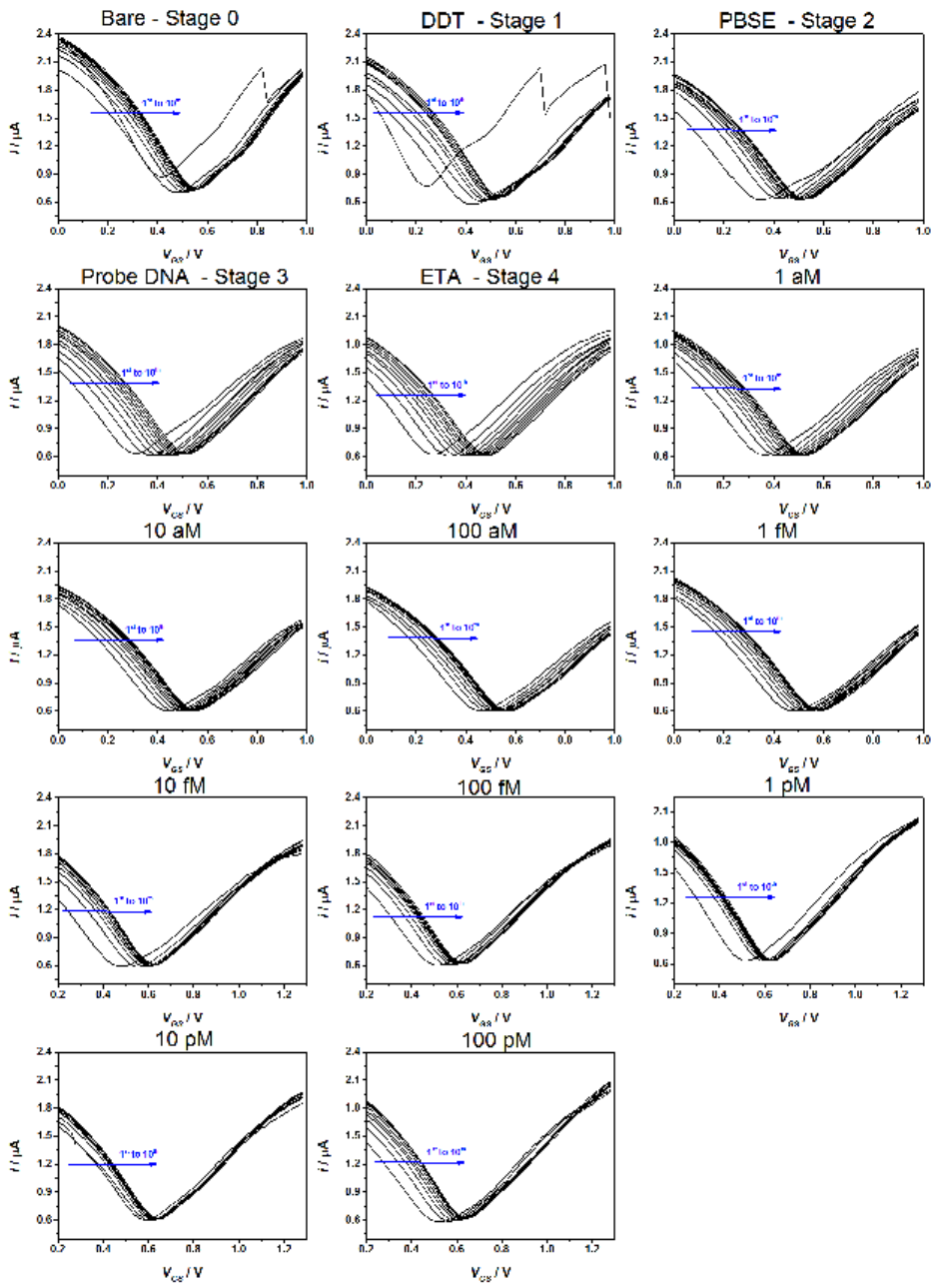

Figure S2 – Complete TC sets for all the stages and different concentrations.

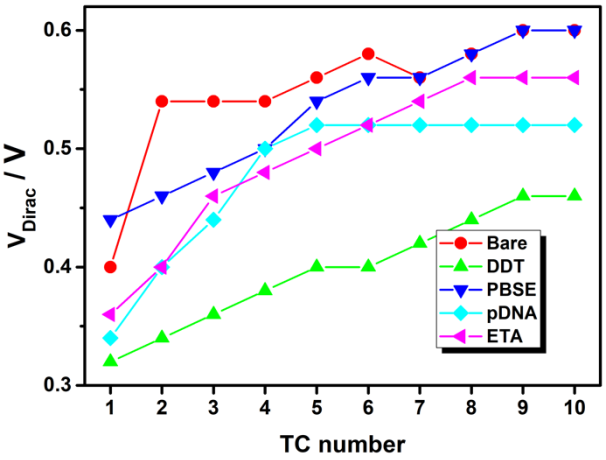

Figure S3. Position of V_{Dirac} as a function of the TC curve number. Curves are numbered sequentially in time.

Raman Characterization

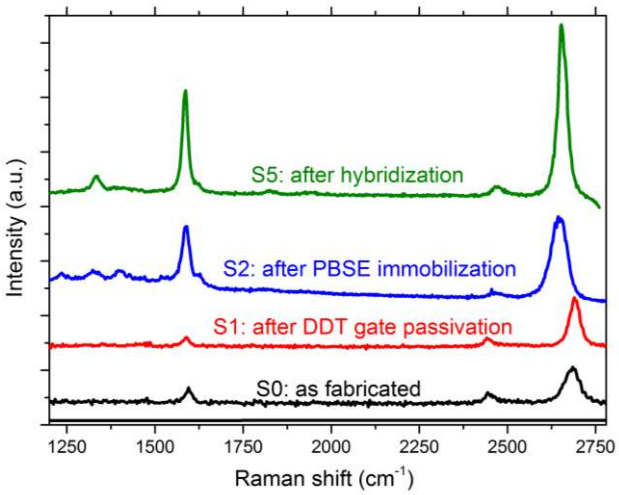

Figure S4 – Characteristic room temperature Raman spectra of the graphene channel of the transistor after stages 0, 1, 2, and 5 of the functionalization/biorecognition process. Spectra S0 and S1 were obtained with 532 nm laser excitation line and S2 and S5 with 633 nm laser line.

Carbon based materials have two distinctive features in their Raman spectra, namely the G mode at ≈ 1580 cm^{-1}, and the 2D mode at ≈ 2700 cm^{-1}. The G mode is the most intense mode in graphitic samples. The 2D mode is a two-phonon double resonance Raman mode and it is the most intense mode in single layer graphene. The 1st order D mode (≈1350 cm^{-1}) is absent in pristine graphene due to the Raman selection rules. If this mode is present, it means that graphene has defects, which breakdown the selection rules. The D intensity is proportional to

the sample defect level.[1,2] The Raman spectrum acquired after stage 0 (Figure S4, black line) shows that the CVD grown graphene is single layer (I2D/IG > 1) with almost no defects, as seen by the absence of the D mode. The passivation of the gate with DDT in stage 1 did not influence the graphene quality as can be seen in the Raman spectrum (Figure S4, red line) where the defect D mode is absent, and is overall a very similar spectrum to the one acquired after stage 0, with a FWHM of the 2D peak of 33 cm^{-1}. However, after the functionalization of the graphene channel with PBSE (stage 2) the Raman spectrum shows some extra features in the range 1200-1400 cm^{-1}. The spectrum has been fitted, using one Lorentzian function for each new contribution, and the fitting spectrum clearly shows two new peaks at ≈ 1235 cm^{-1} and ≈ 1398 cm^{-1}, and the appearance of the D mode. The new peaks are assigned to C-H bending and C=C in-plane vibration modes of the pyrene group, respectively,[3–5] which is part of the PBSE linker. These modes have a larger FWHM than found in pure pyrene. A broadening and a shift in pyrene Raman peak positions was reported in relation with surface effects.[5]

XPS characterization

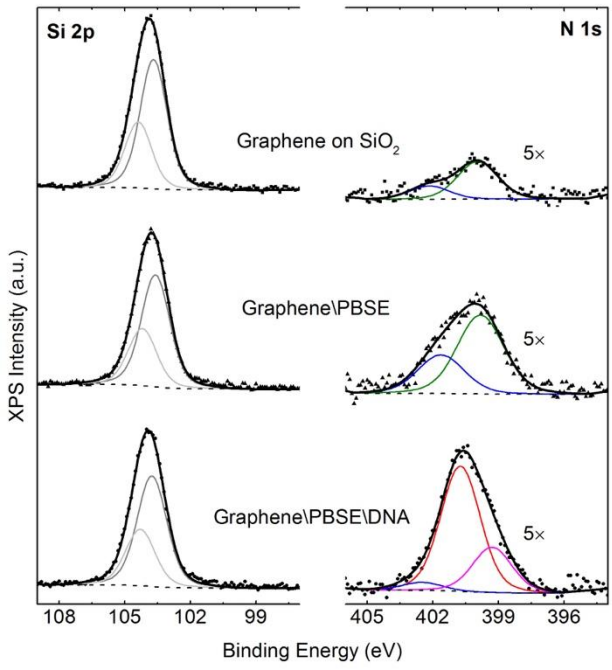

Figure S5 – XPS signatures acquired after individual steps in functionalization of graphene with DNA probes. The S2p 1s (left) and N 1s (right, shown multiplied by a factor of 5) spectral regions are shown for the initial graphene surface on silicon oxide (top), PBSE-modified graphene (middle), and PBSE-modified graphene after immobilization of the simulated DNA probes (bottom). Symbols=raw data; thick lines=overall fits; thin colored lines=fit components; dashed lines=background. The high sensitivity of XPS results in detecting in the N 1s region the small amount of contamination, most likely from polymeric residue, on the initial graphene surface.

Calibration curves

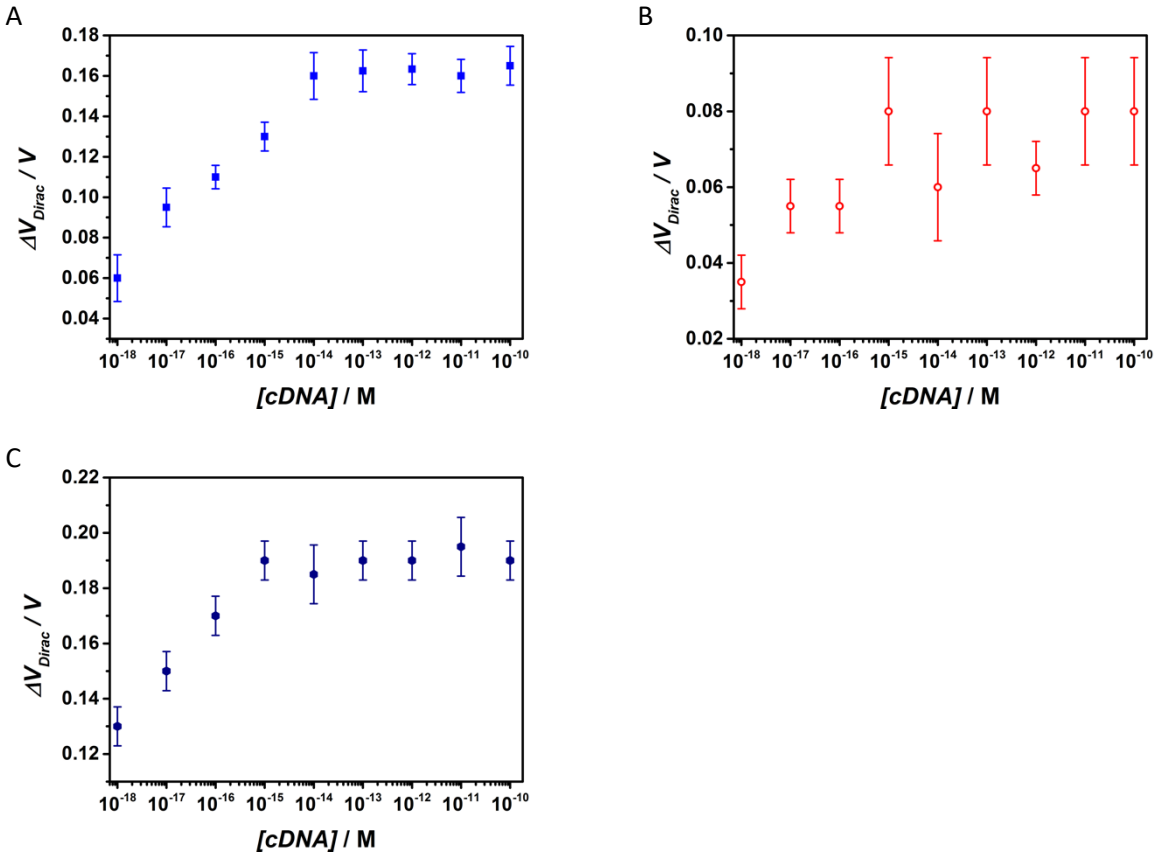

Figure S6 – Calibration curves for the different experiments. A) PM, B) SNP and C) an experiment whose probe DNA was fully complementary to the target named SNP.

Schematic illustration of the molecular system immobilized on graphene, after biorecognition

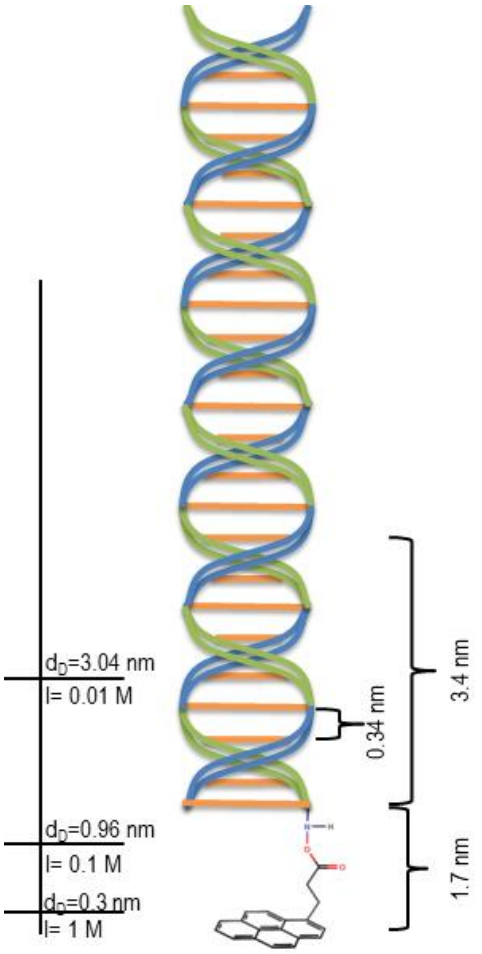

Figure S7. Schematic illustration of a DNA double helix bound to a PBSE linker that links to graphene. Left scale shows Debye length, d_D, as a function of electrolyte ionic strength calculated by Debye-Hückel theory. Right scale shows characteristic molecular lengths.

SEM images of the graphene source, drain and channel area after each biosensor development step

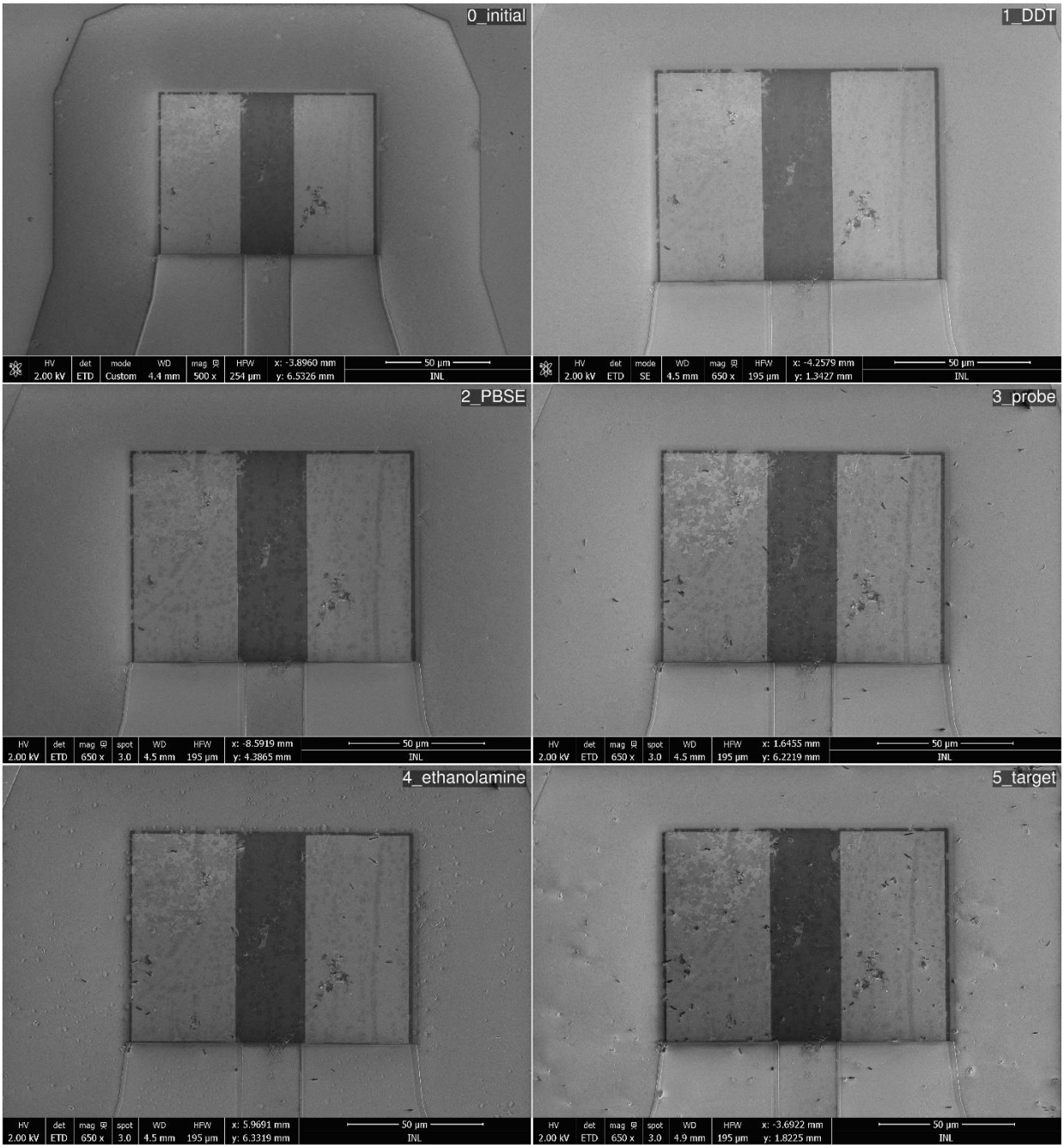

Figure S8 – SEM images of the graphene channel (dark area) of one transistor, in between source and drain Au contacts (clear areas), taken after each of the stages of the biosensor development (see main text and Figure S1). Note that the graphene overlaps the Au S-D contacts, exceeding a few micrometers the Au contact (dark edge). Note: the rectangular source and drain contacts in the images above are slightly different in shape from those shown in the main text (semi-circular).

References

(1) Ferrari, A. C.; Meyer, J. C.; Scardaci, V.; Casiraghi, C.; Lazzeri, M.; Mauri, F.; Piscanec, S.; Jiang, D.; Novoselov, K. S.; Roth, S.; et al. Raman Spectrum of Graphene and Graphene Layers. *Phys. Rev. Lett.* **2006**, *97* (18), 187401 DOI:10.1103/PhysRevLett.97.187401.

(2) Saito, R.; Dresselhaus, G.; Dresselhaus, M. S. *Physical Properties of Carbon Nanotubes*; Published by Imperial College Press and Distributed by World Scientific Publishing Co., 1998.

(3) Shinohara, H.; Yamakita, Y.; Ohno, K. Raman Spectra of Polycyclic Aromatic Hydrocarbons. Comparison of Calculated Raman Intensity Distributions with Observed Spectra for Naphthalene, Anthracene, Pyrene, and Perylene. *J. Mol. Struct.* **1998**, *442* (1–3), 221–234.

(4) Lu, G.; Shi, G. Electrochemical Polymerization of Pyrene in the Electrolyte of Boron Trifluoride Diethyl Etherate Containing Trifluoroacetic Acid and Polyethylene Glycol Oligomer. *J. Electroanal. Chem.* **2006**, *586* (2), 154–160.

(5) Leyton, P.; Gómez-Jeria, J. S.; Sanchez-Cortes, S.; Domingo, C.; Campos-Vallette, M. Carbon Nanotube Bundles as Molecular Assemblies for the Detection of Polycyclic Aromatic Hydrocarbons: Surface-Enhanced Resonance Raman Spectroscopy and Theoretical Studies. *J. Phys. Chem. B* **2006**, *110* (13), 6470–6474.